Barton, P. G., & Gunstone, F. D. (1975) *J. Biol. Chem. 250*, 4470–4476.
Breckenridge, W. C., & Kuksis, A. (1968) *Lipids 3*, 291–300.
Brockerhoff, H., & Yurkowski, M. (1965) *Can. J. Biochem. 43*, 1777.
Büldt, G., Gally, H. U., Seelig, A., Seelig, J., & Zaccai, G. (1978) *Nature (London) 271*, 182–184.
Chapman, D. (1975) *Q. Rev. Biophys. 8*, 185–235.
Chapman, D., Urbina, J., & Keough, K. M. (1974) *J. Biol. Chem. 249*, 2512–2521.
Cubero-Robles, E., & van den Berg, D. (1969) *Biochim. Biophys. Acta 187*, 520–526.
Dawson, R. M. C. (1960) *Biochem. J. 75*, 45–53.
DeKruyff, B., Demel, R. A., Slotboom, A. J., van Deenan, L. L. M., & Rosenthal, A. F. (1973) *Biochim. Biophys. Acta 307*, 1–19.
Dunphy, G. B., Keough, K. M. W., & Nolan, R. A. (1977) *Can. Entomol. 109*, 347–350.
Eliasz, A. W., Chapman, D., & Ewing, D. F. (1976) *Biochim. Biophys. Acta 448*, 220–230.
Fiske, C. H., & Subbarow, Y. (1925) *J. Biol. Chem. 66*, 375–400.
Haberkorn, R. A., Griffin, R. G., Meadows, M. D., & Oldfield, E. (1977) *J. Am. Chem. Soc. 99*, 7353–7355.
Hanahan, D. J. (1952) *J. Biol. Chem. 195*, 199–206.
Hitchcock, P. B., Mason, R., Thomas, K. M., & Shipley, G. G. (1974) *Proc. Natl. Acad. Sci. U.S.A. 71*, 3036–3040.
Ladbrooke, B. D., & Chapman, D. (1969) *Chem. Phys. Lipids, 3*, 304–367.
Ladbrooke, B. D., Williams, R. M., & Chapman, D. (1968) *Biochim. Biophys. Acta 150*, 333–340.
Lee, A. G. (1977a) *Biochim. Biophys. Acta 472*, 237–281.
Lee, A. G. (1977b) *Biochim. Biophys. Acta 472*, 285–344.
Lee, A. G. (1978) *Biochim. Biophys. Acta 507*, 433–444.
Mangold, H. K., & Malins, D. C. (1960) *J. Am. Oil Chem. Soc. 37*, 383–385.
Mabrey, S., & Sturtevant, J. M. (1976) *Proc. Natl. Acad. Sci. U.S.A. 73*, 3862–3866.
Oldfield, E., Meadows, M., Rice, D., & Jacobs, R. (1978) *Biochemistry 17*, 2727–2740.
Phillips, M. C., Ladbrooke, B. D., & Chapman, D. (1970) *Biochim. Biophys. Acta 196*, 35–44.
Phillips, M. C., Hauser, H., & Paltauf, F. (1972) *Chem. Phys. Lipids 8*, 127–133.
Seelig, A., & Seelig, J. (1975) *Biochim. Biophys. Acta 406*, 1–5.
Seelig, J., & Waespe-Šarčevič, N. (1978) *Biochemistry 17*, 3310–3315.
Selinger, Z., & Lapidot, Y. (1966) *J. Lipid Res. 7*, 174–175.
Shimshick, E. J., & McConnell, H. M. (1973) *Biochemistry 12*, 2351–2360.
Singleton, W. S., Gray, M. S., Brown, M. L., & White, J. L. (1965) *J. Am. Oil Chem. Soc. 42*, 53–56.
Smith, M. W. (1976) *Biochem. Soc. Symp. No. 41*, 43–60.
Tardieu, A., Luzzati, V., & Reman, F. C. (1973) *J. Mol. Biol. 75*, 711–733.
Vaughan, D. J., & Keough, K. M. (1974) *FEBS Lett. 47*, 158–161.
Wagner, H., Hörhammer, L., & Wolff, P. (1961) *Biochem. Z. 334*, 175–184.
Wells, M. A., & Hanahan, D. J. (1969) *Methods Enzymol. 14*, 178–184.

Electrostatic Interactions at Charged Lipid Membranes. Electrostatically Induced Tilt†

Fritz Jähnig,*,‡ Karl Harlos, Horst Vogel,‡ and Hansjörg Eibl

ABSTRACT: The changes in bilayer structure induced by surface charges in the case of an ionizable lipid were studied by X-ray diffraction, Raman spectroscopy, and film-balance measurements. With increasing surface charge in the ordered phase, the X-ray results show a decrease in bilayer thickness, whereas the hydrocarbon chain packing stays essentially constant, the Raman data signify that the internal chain ordering does not change, and the monolayer studies show a lateral expansion of the bilayer. These results are interpreted in terms of a tilt of the chains caused by the surface charges on the polar heads. The tilt angle between the direction of the chains and the bilayer normal is obtained by a detailed theoretical evaluation. The tilt allows for a better understanding of the electrostatically induced shift of the phase transition temperature and of the shift induced by the binding of water in the case of lecithin in contrast to ethanolamine.

Since the first studies of lipid membranes it has been known that their properties vary with temperature. There are gradual variations and also an abrupt change is observed, the so-called ordered–fluid transition. In most biological systems, however, temperature is kept constant. Therefore one is interested in other external parameters by which membrane properties can be regulated. Biological membranes may contain up to 20% ionizable lipids. So one is tempted to expect electrostatic surface charges to represent a relevant regulation mechanism. They can be switched on and off when we vary the concentrations of ions in the electrolyte environment and, on the other hand, change the lateral packing of the lipid molecules, i.e., the membrane structure. Electrostatic effects at charged membranes have been studied extensively by use of pure lipids (for a review see Träuble, 1976). It was shown that the ordered–fluid phase transition can be triggered electrostatically, e.g., by varying the external pH at constant temperature. So the electrostatic regulation of membrane properties can be

† From the Max-Planck-Institut für biophysikalische Chemie, 3400 Göttingen, West Germany. *Received May 11, 1978; revised manuscript received October 27, 1978.* This work was supported by the Deutsche Forschungsgemeinschaft through SFB 33 (F.J.).
‡ Present address: Max-Planck-Institut für Biologie, 7400 Tübingen, West Germany.

0006-2960/79/0418-1459$01.00/0

a very sensitive process. The inverse effect was also observed: a change in the lateral packing of the lipid molecules leads to a change in the ionic concentrations of the electrolyte environment; e.g., the spontaneous lateral expansion at the thermal phase transition gives rise to a proton pulse into the electrolyte medium (Woolley & Eibl, 1977; Vaz et al., 1978).

Up to now experiments with ionizable lipids have mainly been devised to detect the ordered–fluid transition. It is clear, however, that surface charges change the bilayer structure also far from the phase transition. Because of their electrostatic repulsion, they induce a lateral expansion of the lipid polar heads. This has been verified by monolayer studies on a film balance (Sacré & Tocanne, 1977). We then have to ask, how do the hydrocarbon chains react on the electrostatic expansion in the plane of the polar heads? To answer this question is the aim of the present paper.

To investigate a bilayer under varying surface charge, i.e., different pH values, we synthesized a lipid which is highly stable against pH changes, dihexadecylphosphatidic acid (DHPA).[1] The hydrocarbon chains of DHPA are linked by ether bonds to the glycerol backbone. Ether-linked lecithins have already been synthesized (Berecoechea et al., 1968) and were investigated on a film balance (Paltauf et al., 1971) and by calorimetry (Vaughan & Keough, 1974). Phosphatidic acid has two dissociable protons; in the case of bilayers the first proton is released between pH 1 and 3 and the second is released between pH 7.5 and 10 (Träuble & Eibl, 1974). We studied phosphatidic acid bilayers at pH 7 and 12 corresponding to one and two negative charges per lipid molecule.

X-ray diffraction is used as one possibility to explore the chain ordering (for a review see Luzzati, 1968). This method allows us to determine the period of the lamellar phase, i.e., the thickness of a lipid plus water layer (long spacings). A change observed in this period may be caused by different effects: a change of (i) the water-layer thickness, (ii) the internal chain conformation which is coupled to the packing density of the chains, and (iii) the orientation of the chains, i.e., the tilt. These effects may also be superimposed. The contribution of the first effect can be determined easily if the water ratio of the lamellar phase is known. The second effect we investigated by high-angle X-ray diffraction (short spacings) and independently by Raman spectroscopy [see Gaber & Peticolas (1977) and also the references cited therein]. The contribution of the third effect we obtained from an evaluation of the X-ray long and short spacings. Monolayer experiments were used as a test of the results from the X-ray long spacings.

Materials and Methods

Lipid Synthesis. 1,2-Dihexadecyl-*sn*-glycerol was purchased from Fluka (Buchs, Switzerland). Phosphorus oxytrichloride was distilled before use, and the fraction, boiling range 105–107 °C, was collected. Solvents were of Baker p.a. grade. The crude reaction product was purified by column chromatography on silica gel HR (Merck, Darmstadt, Germany). Solvent mixtures of chloroform–methanol–ammonia (25% in water) were used for elution. Starting with chloroform–methanol–ammonia, 100:15:1 (v/v), the polarity of the eluent was increased stepwise up to 100:100:30 (v/v) which then eluted 1,2-dihexadecyl-*sn*-glycerol 3-phosphate.

Phosphorus oxychloride (330 mg, 2.2 mmol) was dissolved in 5 mL of trichloroethylene and cooled to 5 °C in an ice bath. By continuous stirring with a magnetic stirrer, a solution of 1,2-dehexadecyl-*sn*-glycerol (1.1 g, 2.0 mmol) and triethylamine (400 mg, 4 mmol) in 10 mL of trichloroethylamine was added dropwise. The reaction mixture was adjusted to 20 °C. After 10 min, starting material was no longer detected by thin-layer chromatography. The reaction mixture was filtered by suction and the filtrate freed from solvent by evaporation under reduced pressure.

The oily residue was taken to 20 mL of tetrahydrofuran (THF), and 10 mL of 2 M sodium acetate was added to hydrolyze the formed 1,2-dihexadecyl-*sn*-glycerol-3-phosphoric acid dichloride. After 2 h, hydrolysis was completed and most of the THF was removed by evaporation under reduced pressure. The remaining water phase was extracted from 10 mL of chloroform in the presence of 12 mL of methanol to facilitate phase separation. Extraction with chloroform was repeated and the combined extracts were evaporated to dryness. The crystalline residue was dissolved in 10 mL of chloroform–methanol–ammonia, 65:15:1 (v/v), and purified by chromatography. The yield of purified product was 1.1 g or 83% based on the dihexadecylglycerol. The structure of the synthesized 1,2-dihexadecyl-*sn*-glycerol 3-phosphate, sodium salt, was confirmed by elemental analysis. Anal. Calcd for $C_{35}H_{71}Na_2O_6P$ (mol wt 664.9): C, 63.22; H, 10.76; P, 4.66. Found: C, 63.07; H, 10.69; P, 4.51.

Sample Preparation for X-ray Studies. In order to work with defined degrees of dissociation or pH at low-water content, different salt forms of DHPA had to be used. For the case of pH 7, 0.5 M phosphoric acid (adjusted to pH 7) was added to the monosodium salt; for pH 12, 0.01 M NaOH (pH 12) was added to the disodium salt.

The different salt forms were obtained in the following manner. A desired amount of lipid was dissolved in a chloroform–methanol–water (1:1.2:1 v/v) mixture and the different phases were properly mixed for 5 min. For the monosodium salt the water again contained 0.5 M phosphoric acid (adjusted to pH 7); to obtain the disodium salt the water contained 0.01 M NaOH (pH 12). After we mixed the phases, the chloroform phase was extracted and dried under a stream of nitrogen, followed by the addition of anhydrous ether. Finally, the lipid was dried in high vacuum ($p < 1 \times 10^{-5}$ torr) for at least 2 h.

For the hydration studies exact amounts of lipid and water (adjusted to pH 7 and 12 in the manner described above) were weighed into glass capillaries. Mixture of water and lipid was achieved by repetitive heating to $T > T_t$ and centrifugation. A glass bead was inserted into the glass capillary to enhance mixture of lipid and water during centrifugation. Then the lipid samples were equilibrated at $T > T_t$ for 0.5–1 h and finally transferred to the X-ray cells. After the measurements, the purity of the lipid was checked by thin-layer chromatography and no degradation was found.

X-ray Camera. The experimental setup of the X-ray diffraction experiments has already been described elsewhere (Harlos, 1978).

Sample Preparation for Raman Spectroscopy. Dry DHPA (40 mg) was swollen in 20 mL of doubly distilled water at a temperature of 70 °C for 1 h. The resultant lipid dispersion with pH 9 was adjusted to pH 7 and 12 by addition of appropriate amounts of 1 M HCl or 1 M NaOH, respectively, vortex mixed for 1 min, and incubated at 70 °C again for 2 h.

To obtain a high-concentrated lipid–water mixture for Raman spectroscopy, the DHPA dispersions were centrifuged with 100000*g* at 15 °C (pH 12 samples were centrifuged for

[1] Abbreviations used: DHPA, dihexadecylphosphatidic acid; DMMPA, dimyristoylmethylphosphatidic acid; LAM, longitudinal acoustic mode; SOM, skeletal optical mode.

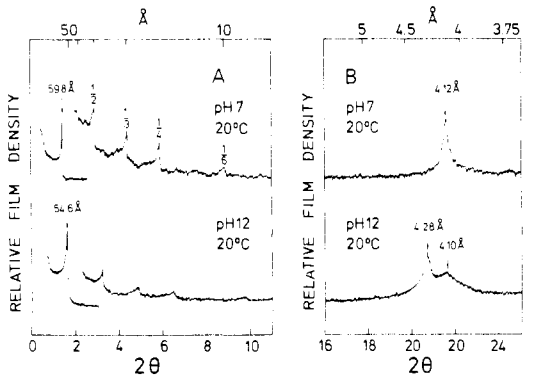

FIGURE 1: X-ray diffraction pattern of DHPA at low (A) and high (B) scattering angles 2θ. Excess water, 20 °C, pH 7 and 12.

6 h and pH 7 samples for 1 h). The pellets with lipid concentration of about 60% were transferred to thin-walled glass capillaries and sealed. (The lipid concentration was determined by weighing the pellet before and after drying in a desiccator with P_2O_5.) The pH of the supernatant was the same as the pH of the starting dispersion. The pH dependence of the phase transition temperature of the pellets determined by Raman spectroscopy was the same as that of diluted (10^{-3} M) dispersions determined by calorimetry and fluorescence indicators (Blume & Eibl, 1978). Therefore the pH in the pellet should agree with the pH in the supernatant.

Raman Spectrometer. The Raman spectrometer consists of an Ar^+ ion laser (Coherent Radiation, Model 52A), operated at a power of 400 mW at 514.5 nm. Raman scattered light was observed at 90° and analyzed with a Jarrel-Ash double monochromator (slit width 220 μm) equipped with an ITT F130 photomultiplier, photon-coupling detection, and a strip chart recorder.

The capillaries were placed in a properly machined variable-temperature cell holder, controlled by flowing water from a Lauda thermostat. The temperature in the sample was measured with a thermocouple inserted in the capillary. A correction for laser heating was determined by continuously monitoring the intensity decrease of the 90° stray light from a DHPA–H_2O mixture at 514.5 nm with the Raman spectrometer as a function of temperature when the lipid dispersion goes from the crystalline to the liquid–crystalline state. The transition temperature of the lipid sample at an excitation power of 400 mW was 3.5 °C higher than the transition temperature observed with a power of 4 mW, where heating effects are assumed to be negligible.

Monolayer Studies. Monolayers were spread when we lowered a droplet of lipid in chloroform on a subphase of doubly distilled water and 0.1 M NaCl whose pH was adjusted to the desired value by addition of 1 M NaOH. Surface pressure-area diagrams were recorded by use of a commercial Langmuir trough (Lauda), Teflon-coated with plexiglass cover. The trough and the nitrogen gaseous phase could be thermostated with an accuracy of ±0.5 °C. After evaporation of the solvent, the film was compressed at a rate of 5 (Å²/molecule)/min. The accuracy of the surface pressure measurement is 2%.

Experimental Results

X-ray Diffraction. The result of a typical X-ray diffraction experiment is shown in Figure 1. At low scattering angles 2θ, Bragg reflections appear corresponding to the one-dimensional order of the lipid–water lamellar phase (long spacings). The reflections are related to the period d of this spatial order through the Bragg condition $2d \sin \theta = n\lambda$, λ being the X-ray wavelength and n being an integer. Up to the sixth order ($n = 6$), reflections are detectable. No superposed reflections were observed, implying the phase to be one-dimensional lamellar (L) and not of the two-dimensional rippled type (P). For the temperature 20 °C and excess water, we found that the period decreases from $d = 59.8$ Å at pH 7 to $d = 54.6$ Å at pH 12.[2]

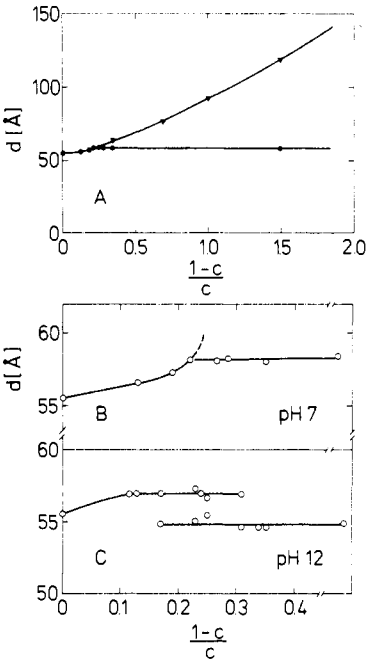

FIGURE 2: Variation of the period d with the water/lipid weight ratio $(1 - c)/c$ at 20 °C. (A) Phosphatidic acid, disodium salt without buffer, according to Ranck et al. (1974) (▼) and DHPA, monosodium salt with 0.5 M phosphate buffer (pH 7) (●); (B) DHPA, monosodium salt with 0.5 M phosphate buffer (pH 7); (C) DHPA, disodium salt with 0.01 M NaOH (pH 12).

At higher scattering angles another group of reflections is observed (short spacings). In the ordered phase they arise from the two-dimensional order of the hydrocarbon chains in a plane perpendicular to the chain axes (called the chain plane). In many cases this order has been found to be hexagonal although higher order reflections are usually very weak (Tardieu et al., 1973). In our measurements only first-order reflections were detected. Again for 20 °C and excess water, at pH 7 we obtained one sharp line with weak shoulders which can be regarded as the superposition of a sharp and a slightly broadened reflection from a hexagonal lattice. The distance s of the scattering planes results, again by use of the Bragg condition, as $s = 4.12$ Å. At pH 12, the first-order reflections are clearly split up into a sharp line at $s = 4.28$ Å and a broad line at $s = 4.10$ Å. The ratio of intensities of the sharp and the broad reflection as determined by decomposition of the two overlapping lines is about 2.

For a quantitative evaluation of these data it is necessary to know the water/lipid ratio in the lamellar phase. This can be obtained from a study of the water uptake in the lamellar phase. It is known that charged lipids usually incorporate water without any limit, as shown in Figure 2A by the data

[2] Recently, the packing of another charged lipid, phosphatidylglycerol, was studied using X-ray diffraction by Ranck et al. (1977). Their findings are quite different from ours for DHPA. From the long spacings they deduced that the bilayer thickness is about half of the usual value (the double molecular length). This and other results led them to conclude that the hydrocarbon chains of the two halves of the bilayer interdigitate. Evidence for a tilt in charged phosphatidylglycerol was obtained by Watts et al. (1978).

Table I: Temperature Dependence of the X-ray Diffraction Spacings of DHPA for $(1 - c)/c = 0.24$

T (°C)	d (Å)	s (Å)
	pH 7	
5	60.3	3.85, 4.18
51	60.0	4.18
62	59.9	4.22
72	59.8	4.27
80	54.3	(broad line)
	pH 12	
4.5	55.6	4.06, 4.30
40	56.2	4.22
47	56.2	4.23
55	56.2	4.25
63	56.5	4.26
	50.9	(broad line)

of Ranck et al. (1974) on phosphatidic acid from hen egg. Since for our aims we had to detect small changes in bilayer thickness, it was advantageous to work with thin water layers. This can be achieved by use of high salt concentrations where high concentration means salt in addition to the sodium ions of the lipid (Gulik-Krzywicki et al., 1969). Then a saturation behavior of the period d is found as shown again in Figure 2A, for DHPA at pH 7. It resembles the familiar results for uncharged lipids like lecithins (Chapman et al., 1967; Tardieu et al., 1973; Janiak et al., 1976): above a certain water/lipid ratio the period d stays constant, additional water forming its own phase (excess water). For pH 7, according to Figure 2B, saturation sets in at 22 ± 1 wt % water/lipid. The preparation of the samples for these measurements was slighly different from the preparation in the case of Figure 1, the incubation time being shorter, and therefore the two values obtained for d at excess water differ slightly. To correct for this deficiency one may extrapolate the experimental curve of Figure 2B to higher values of d; for the water/lipid ratio at saturation, corresponding to d = 59.8 Å (Figure 1), one then gets 24 ± 2%. For pH 12, the initial water uptake shows a more complex behavior (Figure 2C). The period d starts to increase as for the case of pH 7, but in the saturation regime an additional, smaller period appears which then persists up to high water content, whereas the larger period vanishes. The simultaneous existence of two lamellar periods has also been observed with soaps and was described as a coexistence of crystalline and lamellar phases (Vincent & Skoulios, 1966). In our case one may also think of two phases which differ in the ionization of the lipid polar heads (pH 7 and 12). The period d at excess water agrees with the value of Figure 1, but the onset of saturation cannot be fixed exactly. Simple reasoning would lead one to put it into the middle of the double-period region, i.e., at 24% water/lipid. This value signifies that the water uptake is similar for pH 7 and 12, at high salt concentration.

In order to study the temperature variation of the lipid order, especially of the tilt, powder patterns at excess water were recorded for different temperatures, as shown in Figure 3. In the case of pH 7, the period d remains essentially constant in the ordered phase and decreases abruptly at the phase transition which occurs at 72 °C (Blume & Eibl, 1978). The high-angle reflections below 20 °C are split up into two lines; above 20 °C they are superposed. The distance s becomes slightly larger with increasing temperature and the reflection line becomes slightly sharper. These findings suggest a decrease in the tilt angle with increasing temperature. Above the phase transition, a very broad line is observed as known from other lipids. In the case of pH 12, the period d slightly increases with increasing temperature, up to the phase transition at 50 °C. The broad line of the high-angle re-

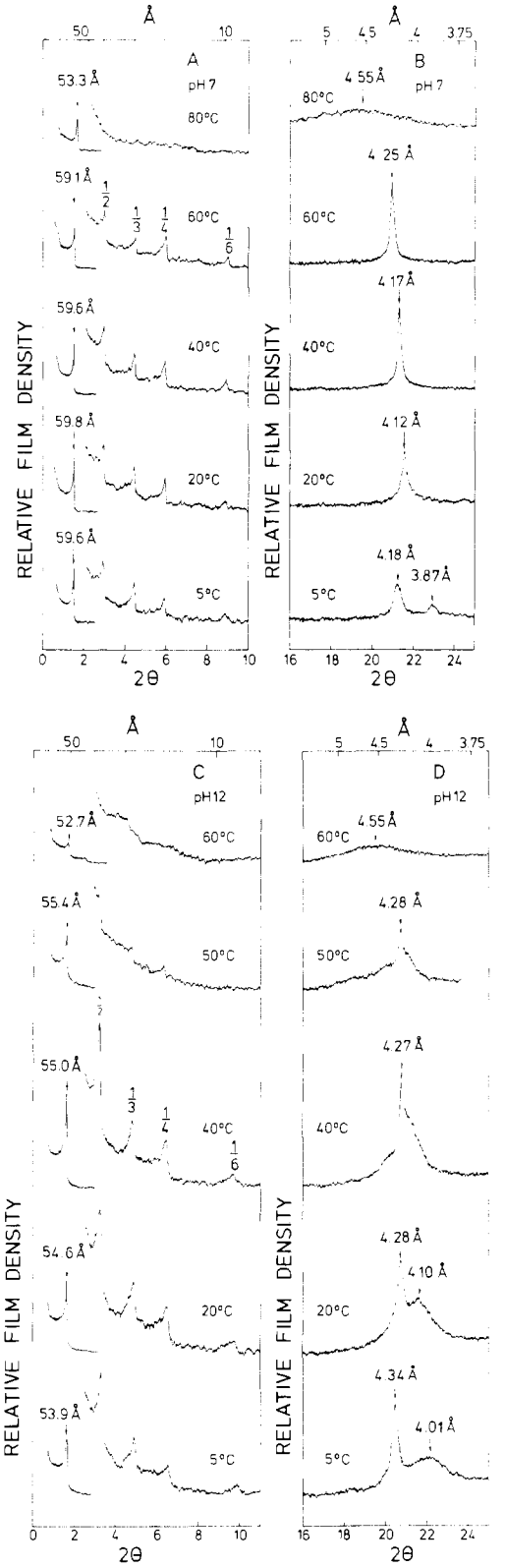

FIGURE 3: Temperature behavior of the X-ray diffraction pattern of DHPA. Excess water, pH 7 (A and B) and pH 12 (C and D).

flections moves to larger distances until the splitting nearly vanishes. A similar temperature behavior of the short spacings has been reported for lecithin (Tardieu et al., 1973; Janiak et al., 1976) and for phosphatidylethanolamine (Harlos, 1978).

We furthermore studied the temperature variation of the X-ray spacings for a fixed water content below or at the saturation value. The qualitative behavior is the same as that for excess water; the values for the long and short spacings

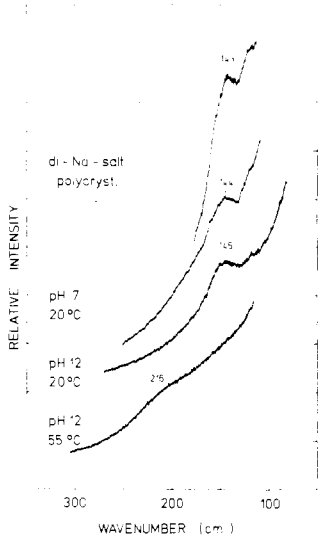

FIGURE 4: Raman spectra of the longitudinal acoustic modes (LAM) of DHPA under different conditions: solid DHPA as disodium salt (upper spectrum) and lipid/water mixtures with $(1 - c)/c = 0.40$ (all other spectra).

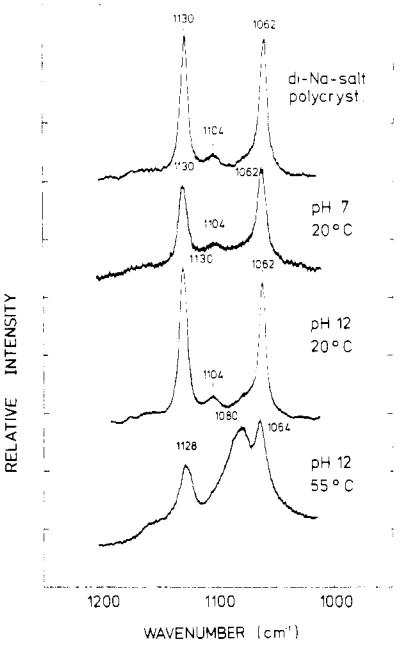

FIGURE 5: Raman spectra of the C–C stretch vibrations (SOM) of DHPA under conditions as in Figure 4.

at different temperatures are given in Table I, for pH 7 and 12 at 24% water/lipid.

Raman Spectroscopy. There are two regions in the Raman spectrum of lipids which are sensitive to changes in the internal chain conformation. Figure 4 shows the low-frequency spectrum of DHPA in the polycrystalline state and in the lamellar phase at 20 °C for pH 7 and 12. In all three spectra a broad peak is present with an apparent maximum between 143 and 145 cm^{-1}. The peak is situated on a sharply decreasing flank of the excitation stray light background and low-frequency water contributions. When we assume a Lorentzian profile for the background, the real band maximum lies between 148 and 150 cm^{-1}. Since this band appears at the same position when we use the 488-nm excitation laser line and since a Raman frequency around 150 cm^{-1} from the glass capillary is lacking, this band originates in a lipid molecule vibration. It has been observed in only a few other lipid systems (Brown et al., 1973; Mendelsohn et al., 1975; Gaber & Peticolas, 1977). The molecular vibration can be specified as the accordion-like vibration of a hydrocarbon chain, the longitudinal acoustic mode (LAM), whose frequency is inversely proportional to the length of the chain or a chain segment in all-trans conformation. The frequency of the real band maximum of Figure 4 for DHPA agrees with the LAM frequency of a hydrocarbon chain with 16 carbon atoms in all-trans conformation,[3] which was observed at 148 cm^{-1} for $CH_3(CH_2)_{14}CH_3$ (Schaufele, 1968). The appearance of the band at 150 cm^{-1} in DHPA thus proves that at least part of the chains exists in the fully extended conformation, but it does not exclude lipid molecules having disordered chains with gauche states.

The extent of the internal chain disorder can be determined from the Raman spectrum in the 1100-cm^{-1} region. In Figure 5 this is shown for DHPA, again in the polycrystalline state and in the lamellar phase at 20 °C for pH 7 and 12. Three bands at 1062, 1104, and 1130 cm^{-1} are found corresponding to C–C stretch vibrations, the skeletal optical modes (SOM) of a hydrocarbon chain in the all-trans conformation (Gaber & Peticolas, 1977).

The two conformation-sensitive regions of the Raman spectrum of DHPA do not change much when the temperature is increased within the ordered phase. When the ordered–fluid transition is passed over, however, modifications arise. In the low-frequency region at 55 °C for pH 12, a very broad band with a maximum at 216 cm^{-1} is observed (Figure 4). This LAM frequency is roughly the same as that found for a hydrocarbon chain with 10–11 carbon atoms in the all-trans form. This result may be explained when a model in which the chains are divided by gauche bonds into frequency-decoupled segments of different lengths is used, the most frequent being all-trans segments of 10–11 carbons. The spectrum in the 1100-cm^{-1} region also changes at the phase transition. The strong all-trans bands at 1062 and 1130 cm^{-1} loose intensity and shift to 1064 and 1128 cm^{-1}, respectively. A new, strong, broad band arises at 1080 cm^{-1}, which is characteristic of chains containing gauche conformations. The SOM frequency at 1128 cm^{-1} is in good agreement with the position of the corresponding vibration at 1127 cm^{-1} found by us in crystalline lauric acid, where again an 11-carbon all-trans chain is present.

In the ordered phase at pH 7 and 12, also in polycrystalline DHPA, a very small contribution of the 1080-cm^{-1} gauche band is still present (Figure 5). But from our results we conclude that the hydrocarbon chain conformation in the ordered phase of DHPA is essentially all-trans and does not change with increasing surface charge (within the experimental error). For another lipid, dimyristoylmethylphosphatidic acid, electrostatically induced changes of the internal chain conformation have been reported (Vogel et al., 1976). An increase of the intensity of the terminal-methyl proton magnetic resonance with pH was observed for phosphatidylethanolamine and interpreted as an increased mobility of the chain termini for higher surface charge (Michaelson et al., 1974).

Monolayer Studies. Surface pressure-area isotherms of DHPA monolayers at 20 °C for pH 7 and 12 are shown in Figure 6. The surface pressure at a fixed area per molecule increases on going from pH 7 to 12, the increase representing the electrostatic surface pressure. Inversely, at fixed surface pressure the area per molecule increases with pH. This lateral

[3] In DHPA, where the hydrocarbon chains are connected to the glycerol backbone by ether bonds, all the carbon atoms of a chain are involved in the accordion-like vibration, in contrast to the situation in diacylglycerol lipids or fatty acids where the carboxyl-group carbon behaves differently from the rest of the chain carbons (Gaber & Peticolas, 1977).

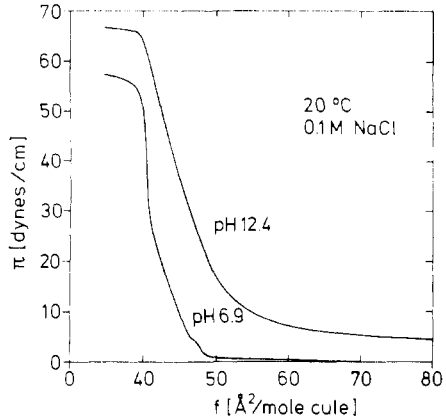

FIGURE 6: Surface pressure-area isotherms of DHPA. Subphase 20 °C, 0.1 M NaCl, pH 7 and 12.

expansion of a monolayer film due to surface charges has already been reported for other ionizable lipids (Sacrê & Tocanne, 1977). At the relatively low temperature of 20 °C no plateau in the surface pressure-area curves of DHPA is observed, which would indicate the ordered–fluid phase transition, as known from other lipids (Paltauf et al., 1971).

Theoretical Evaluation

Method. The tilt angle ϑ can be calculated from X-ray diffraction data by use of the relation (Tardieu et al., 1973)

$$\cos \vartheta = \frac{2f'}{f} \tag{1}$$

where f' is the area of a hydrocarbon chain in the chain plane and f is the area of a lipid molecule in the bilayer plane. f' can be determined from the short spacings and f can be determined from the long spacings by knowledge of the water/lipid weight ratio and the lipid partial volume. Regarding a lipid molecule plus the water per lipid molecule as the tilting unit, whose volume v is given by the sum of the lipid molecular volume v_l and the volume v_w of the water per lipid molecule and whose thickness is equal to half of the period d, one gets

$$f = \frac{v}{d/2} \tag{2}$$

The lipid volume v_l follows from the lipid partial volume ν_l

$$v_l = \frac{M_l}{N_L}\nu_l \tag{3}$$

M_l being the lipid molecular weight and N_L being the Loschmidt number. To determine the water volume, v_w, we note that the water/lipid volume ratio is related to the experimentally known water/lipid weight ratio $(1 - c)/c$ through the partial volumes of lipid and water, ν_l and ν_w, respectively, as

$$\frac{v_w}{v_l} = \frac{\nu_w}{\nu_l}\left(\frac{1-c}{c}\right) \tag{4}$$

Equations 3 and 4 together yield

$$v_w = \left(\frac{M_l}{N_L}\right)\left(\frac{1-c}{c}\right)\nu_w \tag{5}$$

For the case of excess water the saturation value c_s has to be used.

The high-angle scattering data in general show two Bragg reflections with a small difference in the spacings s. The two-dimensional lattice then is a slightly distorted hexagonal lattice, which can be described as a centered rectangular lattice with two perpendicular lattice vectors of length a and b. The area per chain in the chain plane results in $f' = ab/2$. Two of the three manifolds of scattering planes have equal spacings. We attribute to them the index 2, so that the scattering peak corresponding to s_2 is defined to have twice the intensity of the scattering peak corresponding to s_1. When we put s_1 into the [10] direction, then $a = 2s_1$ and by simple geometry $b = s_2(1 - [s_2/(2s_1)]^2)^{-1/2}$, and therefore

$$f' = s_1 s_2\left[1 - \left(\frac{s_2}{2s_1}\right)^2\right]^{-1/2} \tag{6}$$

This allows us furthermore to calculate the average length of a CH_2 monomer along the chain axis as

$$l_{CH_2} = v_{CH_2}/f' \tag{7}$$

which may equivalently be expressed as the stretching factor

$$\xi = l_{CH_2}/l_{CH_2}^0 \tag{8}$$

describing the amount of ordering compared to the fully stretched case with $l_{CH_2}^0 = 1.27$ Å.

Numerical Results. From the data of Figure 1 the tilt angle ϑ for DHPA at 20 °C, pH 7 and 12, will be determined. We start by calculating the area f' from the spacings s_1 and s_2. At pH 7, there is only one peak with $s_1 = s_2 = 4.12$ Å, which yields, by use of eq 6, $f' = 19.6$ Å^2. At pH 12, the 4.28-Å peak has approximately double intensity as compared to the 4.10-Å peak and therefore is indexed 2; i.e., $s_2 = 4.28$ Å and $s_1 = 4.10$ Å, yielding $f' = 20.6$ Å^2. In the chain plane the electrostatic expansion is thus $\delta f'/f' = 5\%$.

To calculate the area f in the bilayer plane, the volumes v_l and v_w of a lipid molecule and the water per lipid molecule, respectively, are needed. Since the measurements of Figure 1 were done at excess water, we have to use for the water/lipid ratios in the lamellar phase the saturation values from Figure 2. As discussed under Experimental Results, we use $(1 - c_s)/c_s = 0.24$ for both pH 7 and 12. From eq 5 with $M_l = 642$ for the monosodium salt of DHPA and $\nu_w = 1$ cm^3 g^{-1}, we obtain for the volume of the water molecules per lipid molecule $v_w = 256$ Å^3.[4]

The calculation of the lipid molecular volume v_l is complicated by the fact that the lipid partial volume ν_l is not known experimentally. Therefore we will determine it by comparison of the DHPA molecule with other lipids. We split up a lipid molecule into the polar head with volume v_p (including the glycerol backbone and the carboxylic groups) and the hydrocarbon chains with volume v_c. The volume of a CH_2 monomer in an ordered chain is known from lecithin to be $v_{CH_2} = 25.5$ Å^3 (Tardieu et al., 1973). A difference between the cases pH 7 and 12 may arise from the fact that the phase transition temperatures for pH 7 and 12 are 72 and 50 °C, respectively; i.e., at 20 °C the lipid chains are 52 and 30 °C below their transition temperatures, respectively. If we assume that the phase transition occurs at the same chain packing density for pH 7 and 12, this temperature difference corresponds to a volume difference due to thermal expansion of $\delta v/v = \gamma \delta T$. With the value $\gamma = 7.48 \times 10^{-4}$ (°C)$^{-1}$ of lecithin

[4] The volume of one water molecule being 30 Å^3, this result means that eight to nine water molecules are bound or trapped by one lipid molecule. The lipid concentration is then as high as 7 M, and since for pH 7 the monosodium salt of DHPA was used the salt concentration is the same. At such high salt concentration the theoretical screening length of the surface charges is about 1 Å, much smaller than the distance between bilayers. The independence of the water-layer thickness from surface charges is therefore conceivable.

(Tardieu et al., 1973) and $\delta T = 22$ °C, one obtains $\delta v/v = 1.7\%$ or $\delta v = 0.4$ Å^3. We will therefore use the values v_{CH_2}(pH 7) = 25.3 Å^3 and v_{CH_2}(pH 12) = 25.7 Å^3, whose average is $v_{CH_2} = 25.5$ Å^3. For later comparison we note that the stretching factor, eq 8, for pH 12 then results in $\xi = 0.98$. The values v_{CH_3} are usually assumed to be twice as large as v_{CH_2}; i.e., v_{CH_3}(pH 7) = 50.6 Å^3 and v_{CH_3}(pH 12) = 51.4 Å^3. This yields for DHPA v_c(pH 7) = 809 Å^3 and v_c(pH 12) = 822 Å^3.

To obtain v_p we compare DHPA with the similar lipid dimyristoylmethylphosphatidic acid (DMMPA) for which the partial volume v_l was measured (Vogel, unpublished experiments), and v_p was found by subtraction of the chain volume v_c from v_l (eq 3). For the monosodium salt of DMMPA the result was $v_p = 233$ Å^3. The differences between the DMMPA and DHPA polar heads are (i) a CH_3 group instead of a proton and (ii) two C=O groups instead of two CH_2 groups. Assuming for (i) 51 − 4 = 47 Å^3 and for (ii) 2[16 − (2 × 4)] = 16 Å^3, we obtain for the monosodium salt of DHPA $v_p = 170$ Å^3. This is half the value for lecithin, $v_p = 340$ Å^3 (Tardieu et al., 1973). An effect due to thermal expansion analogously to the chains will be neglected for the polar heads. For the volume v of a DHPA molecule, including the dissociated Na^+ ion at pH 7, and the water per lipid, we finally get $v = v_p + v_c + v_w = 1235$ Å^3. At pH 12, for the disodium salt with $v_{Na^+} = 20$ Å^3 and $v_{H^+} = 4$ Å^3, the value is slightly higher, $v = 1264$ Å^3.

With these values for v it is straightforward to calculate the tilt angle. When we insert them into eq 2, together with the experimental results for d from Figure 1, the area per molecule in the bilayer plane is obtained as f(pH 7) = 41.3 Å^2 and f(pH 12) = 46.3 Å^2. The electrostatic lateral expansion is thus $\delta f/f = 11\%$, more than twice the expansion in the chain plane. Finally, eq 1 yields for the tilt angle of DHPA at 20 °C ϑ(pH 7) = 18° and ϑ(pH 12) = 27°. This represents our main result: with increasing surface charge the tilt increases. Assuming that in the uncharged case there is no tilt, our finding would indicate a saturation behavior of the tilt at high surface charge, probably due to steric hindrance.

The largest uncertainty in this result arises from the uncertainty in the water uptake, especially for pH 12. If we would have used $(1 - c_s)/c_s = 0.31$, the value at the upper end of the double-period region in Figure 2C, we would have obtained f(pH 12) = 49.0 Å^2 and ϑ(pH 12) = 33°, representing a 20% deviation from the above value. It seems unreasonable to allow for a smaller uptake of water with increasing surface charge, i.e., for a value of $(1 - c_s)/c_s$ smaller than 0.24 for pH 12. Therefore the above result should be regarded as a lower limit for the increase in tilt with surface charge.

Further Evidence for a Tilt. (i) X-ray Line Width. For the above calculation of the tilt angle, only the position of the X-ray reflections was evaluated, i.e., the spacing of the scattering planes. Further information can be obtained from the line width of the high-angle scattering reflections. If the chains are tilted, the number of coherently scattering lattice planes is reduced, leading to a broadening of the scattering peak (Tardieu et al., 1973). For the case of pH 12, Figure 3D clearly shows the 4.10-Å peak to be broadened, which indicates that the chains are tilted. At pH 7, there is also an indication of a broadening of one of the three superimposed reflections, but a weaker broadening, i.e., a smaller tilt, in agreement with the quantitative results above.

Since the Bragg reflection of low intensity (indexed 1) is broadened, the direction of the tilt in the bilayer plane is perpendicular to one manifold of scattering planes and lies in the [10] direction of the centered rectangular lattice, as illustrated in Figure 7. In Figure 7B we have drawn for comparison the lattice in the chain plane, as determined from the short spacings, and its projection into the bilayer plane, for the calculated tilt angle and the [10] tilt direction, both for pH 12. In addition, we show in Figure 7A the lattices in the bilayer plane for pH 7 and 12. A simple picture emerges: the lattice in the plane of the polar heads at pH 7 is hexagonal-like with a slight elongation in the [10] direction; under the action of additional surface charges it expands isotropically; the chains try to reduce the change in their packing density by tilting; and they tilt into the [10] direction in which their packing density without tilt would be minimal.

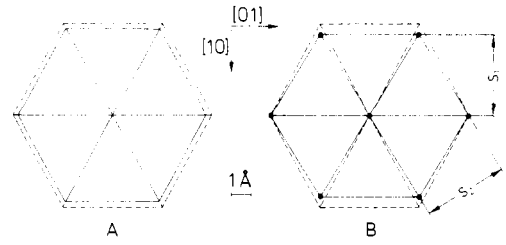

FIGURE 7: The variation of the chain packing with pH for DHPA at 20 °C. (A) The lateral expansion in the bilayer plane on varying the pH from pH 7 (—) to pH 12 (---); (B) the decrease of the area per chain for pH 12 going from the bilayer plane (---) to the tilted chain plane (—).

(ii) Raman Spectroscopy. The constancy of the interchain distance on changing the surface charge as deduced from the X-ray data implies the constancy of the chain conformation. As discussed already, this was verified by Raman spectroscopy: (1) the LAM frequency, depending on the all-trans chain length, does not change with pH and (2) the intensities of the SOM bands indicate a high internal chain order at both pH 7 and 12.

The latter result can be quantified. According to Gaber & Peticolas (1977), the probabilities P_t and P_g for a C–C bond occurring in a trans or a gauche conformation, respectively, are proportional to the intensities I_t and I_g of the 1062- and 1080-cm^{-1} stretch vibration bands, respectively. The simple relation

$$\frac{P_t}{P_g} = \alpha \frac{I_t}{I_g} \tag{9}$$

allows us to calculate the ratio of trans and gauche conformations if the intensities can be determined from the observed spectra and the proportionality constant α by a properly chosen reference state. It was possible to fit the spectra of Figure 5 by a superposition of Lorentzians (Vogel, 1978) and thus to obtain I_t and I_g. As the reference state to fix α we chose the fluid phase of DHPA at 55 °C, pH 12, and attributed to it the value $P_t = 0.69$, as calculated by Schindler & Seelig (1975) within Marcelja's model for lipid bilayers. The spectra of DHPA in the ordered phase at 20 °C could then be evaluated. For pH 12, using eq 9 we obtained $P_t = 0.95$. This result again states that the hydrocarbon chains in the ordered phase of DHPA, even for high surface charge, are essentially in the all-trans conformation.

It is possible to compare the Raman result with the result on average chain length deduced from the X-ray data. We assume that the gauche states in the ordered phase appear only in the form of kinks, i.e., gtg conformations. One kink reduces the chain length by $l_{CH_2}{}^0$, and the stretching factor defined in eq 8 can be expressed as

$$\xi = 1 - \tfrac{1}{2}P_g = \tfrac{1}{2}(1 + P_t) \tag{10}$$

Table II: Temperature Dependence of the Packing Parameters of DHPA for $(1 - c)/c = 0.24$

T (°C)	v (Å^3)	f (Å^2)	f' (Å^2)	ϑ (deg)
		pH 7		
5	1226	40.7	19.2	19
51	1254	41.8	20.2	15
62	1260	42.1	20.6	12
72	1266	42.3	21.1	6
80	1290	47.5		
		pH 12		
4.5	1255	45.1	20.6	24
40	1276	45.4	20.6	25
47	1281	45.6	20.7	25
55	1286	45.8	20.9	24
63	1290	45.7	21.0	23
	1306	51.3		

Inserting the Raman value for P_t at pH 12 yields $\xi = 0.98$, in agreement with the result obtained from the X-ray data.

(iii) Monolayer Studies. The area f per lipid molecule in the bilayer plane is identical with the area per molecule of a monolayer film exposed to an external surface pressure which agrees with the surface pressure acting in a bilayer. Unfortunately, we do not know this bilayer surface pressure. Therefore, to compare our values for f calculated from the X-ray diffraction data with the monolayer data, we first have to use the latter to determine the bilayer surface pressure. The calculated area for pH 7 and 20 °C, $f = 41.3$ Å^2, corresponds in Figure 6 to a surface pressure of $\Pi = 27$ dyn cm^{-1}. At this surface pressure, on the other hand, the area per molecule observed at pH 12 for the monolayer is $f = 47.1$ Å^2. This result agrees within the experimental error with the value derived from the X-ray data, $f = 46.2$ Å^2; it is not compatible with the X-ray value $f = 49.0$ Å^2 obtained if we would allow for a higher water uptake at pH 12. So the monolayer results can be regarded as an experimental justification of our choice of the water uptake at pH 12.

Temperature Dependence. Since the water uptake has not been determined for different temperatures (it may, however, vary with temperature), we used the X-ray data at constant water content below or at the saturation value to evaluate the temperature dependence of the tilt angle. To take into account thermal expansion we applied the thermal expansion coefficient of lecithin, $\gamma = 7.48 \times 10^{-4}$ (°C)$^{-1}$ (Tardieu et al., 1973), to the volume v_c of a hydrocarbon chain, thermal expansion of the polar heads and water being neglected. The X-ray data of Table I were then evaluated as above for 20 °C and lead to the results presented in Table II.

The first conclusion is that the areas f' or the chain packing densities just below the phase transitions for pH 7 and 12 agree within the experimental error, $f' = 21.0$ Å^2, showing that the phase transition in both cases occurs at the same packing density.

The result for the tilt angle in the ordered phase is plotted in Figure 8. At pH 12, ϑ does not vary much with temperature. This may be a consequence of the saturation behavior of the tilt angle at high surface charge mentioned above. For pH 7, ϑ decreases with increasing temperature; whether or not it goes to zero cannot be decided from our results. Since the tilt represents a certain type of long-range order, one would expect ϑ to decrease with increasing temperature up to a second-order phase transition at T_c where it vanishes, but T_c does not have to coincide with T_t. Very similar results for the temperature variation of the tilt angle are obtained in the case of excess water from the data of Figure 3 if we assume that the water uptake does not change with temperature in the ordered phase. The latter is known to hold for lecithin (Janiak et al., 1976), and we conclude that the charged lipid DHPA behaves similarly.

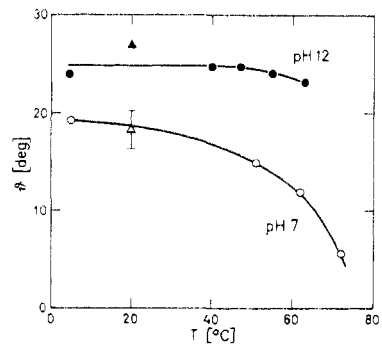

FIGURE 8: Temperature dependence of the tilt angle for DHPA. $(1 - c)/c = 0.24$, pH 7 (○) and pH 12 (●), and excess water, pH 7 (△) and pH 12 (▲).

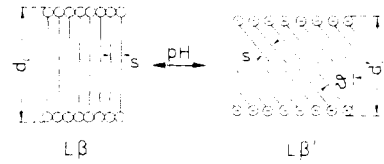

FIGURE 9: Schematic representation of the electrostatically induced tilt. When we switch on the surface charges, the interchain distance s stays constant, the tilt angle ϑ increases, and the bilayer thickness d_l decreases.

In the fluid phase, a tilt angle cannot be determined from our experimental results since the area f' in the chain plane cannot be calculated from the broad high-angle scattering line in the fluid phase (Figure 3B,D). The area f in the bilayer plane, however, can still be derived from the long spacings. We use the values $v_{CH_2} = 27$ Å^3 and $v_{CH_3} = 54$ Å^3 of lecithin to calculate the chain volume. From the data of Table I we obtain the results given in Table II. Comparing the areas f above and below the phase transition, one finds for the spontaneous lateral expansion at the phase transition $\Delta f = 5.2$ Å^2 at pH 7 and $\Delta f = 5.6$ Å^2 at pH 12, for $(1 - c)/c = 0.24$. To deduce the values Δf in the case of excess water, we note that the water molecules which are incorporated in the lamellar phase just before saturation is reached have no detectable influence on the bilayer thickness (Gottlieb & Eanes, 1974). So even if for excess water the number of incorporated water molecules increases at the phase transition, these additional water molecules should not change the bilayer properties, and we are lead to the conclusion that the spontaneous lateral expansion for excess water is approximately the same as that for $(1 - c)/c = 0.24$.

Discussion

The results obtained show that with increasing surface charge on a lipid bilayer the lateral packing of the polar heads decreases. The hydrocarbon chains, in the ordered phase, only partially follow this expansion, due to their attractive van der Waals interaction. In order to minimize a change in packing, they tilt, thereby decreasing the bilayer thickness. This tilt mechanism is illustrated in Figure 9. So, for the first time, we have demonstrated well-defined changes in the bilayer structure induced electrostatically far from the ordered–fluid phase transition.

It is evident that these structural changes influence the ordered–fluid transition. Due to their labilizing effect they decrease the transition temperature T_t, which implies that within a critical temperature range the phase transition can be triggered electrostatically. The electrostatic shift of T_t is

the sum of different effects: a decrease, δT_t, due to the structural changes and a decrease, ΔT_t, arising from a change in the electrostatic field at the phase transition, which is a consequence of the spontaneous lateral expansion, Δf, of the bilayer at the phase transition. The latter mechanism has been investigated theoretically in detail (Jähnig, 1976; Träuble et al., 1976; Forsyth et al., 1977) and was found to be given by $\Delta T_t = -70.7\ \Delta f/f$ [°C] for the effect of one charge per lipid molecule. When we insert for pH 12 our above result, $\Delta f/f = 0.12$, we obtain $\Delta T_t = -9$ °C. This value is too small to account for the experimentally observed shift of −22 °C for DHPA between pH 7 and 12 at excess water. The structural effect has to contribute $\delta T_t = -13$ °C. So the two shift effects are of comparable magnitude, the structural effect being slightly larger, in agreement with an earlier estimate (Jähnig, 1976).

In principle, a change in chain packing density as well as a tilt shifts the phase-transition temperature (Jähnig, 1978, 1979). But since the phase transition for pH 7 and 12 occurs at the same packing density, only the tilt contributes to the structural shift effect. On tilting, a chain at its end looses interaction with a neighboring chain; the noninteracting part of length d_f becomes fluid, and the effective chain length (undergoing the ordered–fluid transition) is reduced. Simple geometry yields approximately $d_f = s_1 \tan \vartheta$ and inserting our results for s_1 and ϑ just below the phase transition (Table I and II), we find d_f(pH 7) = 0.45 Å and d_f(pH 12) = 1.8 Å. The difference in cooperative CH_2 groups between pH 7 and 12 results in $\delta N = \delta d_f / l_{CH_2}^0 = -1.1$. Assumption of a linear dependence of T_t on N with $dT_t/dN = 9$ °C, obtained from the lecithin homologues (Mabrey & Sturtevant, 1976), finally yields $\delta T_t = -10$ °C, in reasonable agreement with the expected value of −13 °C.

A similar reasoning can be applied to the latent heat Q of the phase transition. The contribution of the electrostatic field energy is negligibly small. The tilt effect with the above δN and $dQ/dN = 1.8$ kcal/mol (Mabrey & Sturtevant, 1976) results as $\delta Q = -2.0$ kcal/mol for the difference between the latent heats at pH 7 and 12. This value again agrees well with the experimental result $\delta Q = -2.5$ kcal/mol (Blume & Eibl, 1978). The decrease of latent heat at the phase transition must have its counterpart in an uptake of thermal energy on creating the tilt, i.e., on changing the pH, which has not yet been observed.

One is tempted to generalize the concept of a tilt to other cases of lateral expansion. As a further example we propose the expansion due to binding of water to lecithin. The lecithin polar head covers approximately the area of the two hydrocarbon chains. If water is incorporated between the polar heads, the bilayer has to expand. The result is a tilt, increasing with water content. This is known experimentally, the tilt angle reaching a limiting value of about 25° at maximum hydration (Tardieu et al., 1973; Janiak et al., 1976). By following the above arguments we find that this corresponds to a reduction in effective chain length of $\delta N = -2.0$ and a corresponding shift in transition temperature of $\delta T_t = -18$ °C, induced by the binding of water molecules to the polar heads of lecithin. This value is in agreement with the experimental value obtained from low-angle X-ray diffraction studies (Gottlieb & Eanes, 1974).

Furthermore, one may assume lecithin at vanishing water content, i.e., without tilt, to be equivalent to ethanolamine which is generally supposed not to show a tilt at any water content. The difference in the transition temperature of ethanolamine and lecithin at high water content would then be a consequence of the tilt in lecithin and would be estimated again as −18 °C. The experimental value is −22 °C (Vaughan & Keough, 1974). Analogously, the latent heat would be expected to decrease by −3.4 kcal/mol on going from ethanolamine to lecithin. Experimentally, however, it stays rather constant, indicating that the decrease due to the tilt is cancelled by further effects, probably head-group interactions. Our final conclusion is that the tilt mechanism is a rather general concept for the response of a lipid bilayer to variations in the lateral packing density.

Acknowledgments

We thank A. Nicksch and U. Sievers for providing us with the monolayer data and H. Füldner for helpful discussions.

References

Berecoechea, J., Faure, M., & Anatol, J. (1968) *Bull. Soc. Chim. Biol. 50*, 1561–1567.
Blume, A., & Eibl, H. (1978) (in press).
Brown, K. G., Peticolas, W. L., & Brown, E. (1973) *Biochem. Biophys. Res. Commun. 54*, 358–364.
Chapman, D., Williams, R. M., & Ladbrooke, B. D. (1967) *Chem. Phys. Lipids 1*, 445–475.
Forsyth, P. A., Marcelja, S., Mitchell, D. J., & Ninham, B. W. (1977) *Biochim. Biophys. Acta 469*, 335–344.
Gaber, B. P., & Peticolas, W. L. (1977) *Biochim. Biophys. Acta 465*, 329–340.
Gottlieb, M. H., & Eanes, E. D. (1974) *Biophys. J. 14*, 335–342.
Gulik-Krzywicki, T., Tardieu, A., & Luzzati, V. (1969) *Mol. Cryst. Liq. Cryst. 8*, 285–291.
Harlos, K. (1978) *Biochim. Biophys. Acta 511*, 348–355.
Jähnig, F. (1976) *Biophys. Chem. 4*, 309–318.
Jähnig, F. (1978) *Ann. Phys. (Paris) 3*, 291–296.
Jähnig, F. (1979) *J. Chem. Phys.* (in press).
Janiak, M. J., Small, D. M., & Shipley, G. G. (1976) *Biochemistry 15*, 4575–4580.
Luzzati, V. (1968) in *Biological Membranes* (Chapman, D., Ed.) pp 71–123, Academic Press, London.
Mabrey, S., & Sturtevant, J. M. (1976) *Proc. Natl. Acad. Sci. U.S.A. 73*, 3862–3866.
Mendelsohn, R., Sunder, S., & Bernstein, H. J. (1975) *Biochim. Biophys. Acta 413*, 329–340.
Michaelson, D. M., Horwitz, A. F., & Klein, M. P. (1974) *Biochemistry 13*, 2605–2612.
Paltauf, F., Hauser, H., & Phillips, M. C. (1971) *Biochim. Biophys. Acta 249*, 539–547.
Ranck, J. L., Mateu, L., Sadler, D. M., Tardieu, A., Gulik-Krzywicki, T., & Luzzati, V. (1974) *J. Mol. Biol. 85*, 249–277.
Ranck, J. L., Keira, T., & Luzzati, V. (1977) *Biochim. Biophys. Acta 488*, 432–441.
Sacrê, M. M., & Tocanne, F. J. (1977) *Chem. Phys. Lipids 18*, 334–354.
Schaufele, R. F. (1968) *J. Chem. Phys. 49*, 4168–4175.
Schindler, H., & Seelig, J. (1975) *Biochemistry 14*, 2283–2287.
Tardieu, A., Luzzati, V., & Reman, F. C. (1973) *J. Mol. Biol. 75*, 711–733.
Träuble, H. (1976) in *Structure of Biological Membranes* (Abrahamsson, S., & Pascher, I., Eds.) pp 509–550, Plenum Press, New York.
Träuble, H., & Eibl, H. (1974) *Proc. Natl. Acad. Sci. U.S.A. 71*, 214–219.
Träuble, H., Teubner, M., Woolley, P., & Eibl, H. (1976) *Biophys. Chem. 4*, 319–342.

Vaughan, D. J., & Keough, K. M. (1974) *FEBS Lett. 47*, 158–161.
Vaz, W. L. C., Nicksch, A., & Jähnig, F. (1978) *Eur. J. Biochem. 83*, 299–305.
Vincent, J. M., & Skoulios, A. (1966) *Acta Crystallogr. 20*, 432–440.
Vogel, H. (1978) Dissertation, Göttingen.
Vogel, H., Stockburger, M., & Träuble, H. (1976) *Proc. Int. Conf. Raman Spectrosc., 5th*, 176–177.
Watts, A., Harlos, K., Maschke, W., & Marsh, D. (1978) *Biochim. Biophys. Acta 510*, 63–74.
Woolley, P., & Eibl, H. (1977) *FEBS Lett. 74*, 14–16.

Use of Phosphorus-31 Nuclear Magnetic Resonance to Distinguish Bridge and Nonbridge Oxygens of Oxygen-17-Enriched Nucleoside Triphosphates. Stereochemistry of Acetate Activation by Acetyl Coenzyme A Synthetase†

Ming-Daw Tsai

ABSTRACT: Adenosine 5′-(thiophosphate) (AMPS) contains a prochiral phosphorus center. Differentiation of the two diastereotopic oxygens would allow elucidation of the stereochemical course of biological adenylyl transfer reactions. A general method was developed to distinguish between the "pro-*R*" and "pro-*S*" oxygens. When we converted the AMPS to the isomer A of adenosine 5′-(1-thiotriphosphate) (ATPαS), which is known to have *S* configuration at P_α, the pro-*R* oxygen is incorporated into the bridge position, whereas the pro-*S* oxygen is located at the nonbridge position. The ^{31}P NMR spectra of the ^{17}O-enriched compounds were used to distinguish between the bridge and nonbridge oxygens based on the decrease in the peak intensity of ^{31}P NMR signals caused by the directly bound ^{17}O isotope. The method was used to elucidate the stereochemical course of acetate activation catalyzed by yeast acetyl coenzyme A (CoA) synthetase. The results indicate that yeast acetyl-CoA synthetase is specific for the isomer B of ATPαS and that the nucleophilic displacement proceeds with net inversion of configuration at P_α of ATPαS (B), supporting the "in-line" mechanism.

Adenylyl transfer reactions involve nucleophilic displacement of the pyrophosphoryl group of ATP by the second substrate (Scheme I). In most cases the functional group which undergoes nucleophilic displacement contains oxygen, e.g., carboxyl, hydroxyl, and imidol [HN=C(OH)NH–] groups, or sulfate. This type of reaction is involved in many classes of important biological processes (Stadtman, 1973), e.g., carboxyl group activation (fatty acyl-CoA synthetases, aminoacyl-tRNA synthetases, lipoate activating enzymes, biotin activating enzymes, etc.), biosynthesis of phosphodiester derivatives of adenosine (RNA polymerases, adenylation of amino glycoside antibiotics, etc.), synthesis of adenosine diphosphate derivatives (NAD, FAD, ADPglucose, etc.), sulfate activation, synthesis of imidol adenylate derivatives, and adenylylation of functional groups of proteins. In many cases a third substrate displaces the AMP moiety, resulting in the incorporation of an oxygen from the second substrate into the phosphoryl group of AMP.

Among the numerous enzymes catalyzing reactions involving chiral, prochiral, or proprochiral phosphorus centers, only a few have been analyzed unequivocally for their steric courses, and only two of them, e.g., DNA-dependent RNA polymerase (Eckstein et al., 1976) and tRNA nucleotidyltransferase (Eckstein et al., 1977), are adenylyl transfer reactions. Both enzymes specifically incorporate the isomer A of ATPαS.[1] In both cases, the configuration of the thiophosphate diester bond

Scheme I

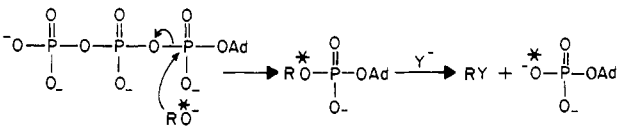

was determined by correlation, through a combination of ribonuclease and chemical reactions, with the endo isomer of uridine 2′,3′-*O*,*O*-thiophosphate, the absolute configuration of which had been determined by X-ray crystallography (Eckstein, 1975). Following elucidation of the absolute configuration of ATPαS (A) (Burgers & Eckstein, 1978), it is now known that both enzymes catalyze the adenylyl transfer reactions with net inversion of configuration at P_α.

In this paper[2] a general method to elucidate the stereochemical course of adenylyl transfer reactions is presented. The method is based on the following rationale. If one of the two isomers of ATPαS is used as a substrate, the stereochemical course of the nucleophilic displacement can be elucidated by determining whether the labeled oxygen of the second substrate is incorporated into the pro-*R* or pro-*S* position of the product AMPS. By converting the AMPS to

† From the Department of Medicinal Chemistry and Pharmacognosy, School of Pharmacy and Pharmacal Sciences, Purdue University, West Lafayette, Indiana 47907. *Received November 28, 1978.* This work was supported by a grant from the Purdue Cancer Research Committee and in part by National Institutes of Health Research Grant GM 18852.

[1] Abbreviations used: AMPS, adenosine 5′-(thiophosphate); ADPαS, adenosine 5′-(1-thiodiphosphate); ATPαS, adenosine 5′-(1-thiotriphosphate); AMP, adenosine 5′-phosphate; ATP, adenosine 5′-triphosphate; Hepes, 4-(2-hydroxyethyl)-1-piperazineethanesulfonic acid; PEP, phosphoenol pyruvate.

[2] An abstract of part of this work has been submitted for presentation at the 177th National Meeting of the American Chemical Society to be held in Honolulu, HI, April 1979.

0006-2960/79/0418-1468$01.00/0